Green Chemistry

Accepted Manuscript

This article can be cited before page numbers have been issued, to do this please use: K. Wang, P. Jiang, M. Yang, P. Ma, J. Qin, X. Huang, L. Ma and R. Li, *Green Chem.*, 2019, DOI: 10.1039/C9GC00908F.

ROYAL SOCIETY OF CHEMISTRY

rsc.li/green-chem

ROYAL SOCIETY OF CHEMISTRY View Article Online
DOI: 10.1039/C9GC00908F

Journal Name

ARTICLE

The metal-free nitrogen-doped carbon nanosheets: a catalyst for directly synthesis imines under mild conditions

Received 00th January 20xx,
Accepted 00th January 20xx

DOI: 10.1039/x0xx00000x

www.rsc.org/

Kaizhi Wang[a,b], Pengbo Jiang[a,b], Ming Yang[a,b], Ping Ma[a,b], Jiaheng Qin [a,b], Xiaokang Huang[a,b], Lei Ma[a,b], and Rong Li*[a,b]

A highly stable, porous multifunctional and metal-free catalyst was explored to exhibit a remarkable catalytic performance in the oxidation of amines and transfer hydrogenation of nitriles reaction under the mild conditions, which was owing to the plenty of active sites and outstanding BET surface area. The results showed that most of the yields of imines were over 90 %, and the cycling performance of the catalyst could be at least seven runs without reaction activity decay, which could be comparable with those metal catalysts. Subsequently, the kinetic study was demonstrated that the apparent activation for the direct synthesis of imine from amine is 67.39 kJ/mol, which also performed to testify the catalytic performances were rational. Through the catalyst characterizations and experimental data, graphitic-N has been proven to be the active sites of the catalyst. Hence, the work is beneficial to comprehend the mechanism of the metal-free N-doped carbon catalyst for resultant imines.

1. Introduction

So far, a great diversity of carbon materials are being developed for the applications, i.e., applying to industrial catalysis, super-capacitor, electro-catalysis and so on.[1] As is well known, whether a carbon material owns outstanding performance depends on the framework construction, such as activated carbon[2], carbon nanotubes (CNTs)[3, 4], graphene oxide (GO)[5], microporous carbon[6], and doped heteroatoms (e.g., B[7, 8], N[9-15], O[16], P[17, 18], and S[15, 19]) into carbon. In particular, the doping of N heteroatoms in carbon materials has attracted extensive research. It is recognized that the atomic radii, bond length, and coordination ability of carbon atoms and heteroatoms are different, which leads to the generation of plentiful defect sites, changes in electron delocalization, and transforms in electronic properties.[20-22] Meanwhile, carbon materials own greatly stable and eco-friendly performance, and thereby it is the good choice for industry as heterogeneous catalysts. Therefore, highly efficient green metal-free carbon-based

[a] State Key Laboratory of Applied Organic Chemistry (SKLAOC).[b] College of Chemistry and Chemical Engineering, Lanzhou University, Lanzhou 730000, PR China. E-mail: liyirong@lzu.edu.cn; Fax: +86-931-891-2582; Tel: +86-18919803060

View Article Online
DOI: 10.1039/C9GC00908F

catalysts should be widely used in industrial processes. For example, the replacement of today's noble metal (Pd-C[23] or Ru-C[24]) heterogeneous catalysts with metal-free catalysts can significantly eliminate the environmental pollution problems caused by metal leaching in the pharmaceutical and petroleum industry. Importantly, the significantly catalytic characteristics of formerly reported N-doped carbon materials could guarantee that their catalytic effect were comparable to the metal doped catalysts.[25-27] Recently, the metal-free mesoporous carbon synthesized from macrocyclic compounds provided by Chen[28] has undergone a cumbersome and toxic preparation process using silica colloid as a template. And the disadvantage of the oxygen-rich carbon quantum dots reported by Ye[16] as a catalyst was that the synthetic process was not in line with the theme of green chemistry. In a word, although these reported catalysts have good results for the conversion of benzylamine to imine, it is necessary to explore a more economical and environmentally friendly catalytic reaction system. Hence, two-dimensional mesoporous N-doped carbon (NC) has been designed to direct synthesis of imines from amines and transfer hydrogenation of nitriles, respectively.

As mentioned above, the NC materials could be applied to synthesize more significant chemical compounds that contained C=N bonds, which were called imines. Imines are a crucial classification of nitrogen sources, since it can be farther employed as functional organic products, liking dyestuffs, chemisterilants, polymers, medicines, and natural products.[28-30] Therefore, applications and synthetic routes of imines are fundamentally demanding research subjects in the chemistry field.[31-33] Generally speaking, imines are formed by the oxidation of alcohols and amines[29, 34], the self-oxidation of primary amines[16, 35], and the self-oxidation of second amines[36], these are the economical, efficient, green and sustainable synthesis methods. In addition, the self-oxidation of primary amines are usually catalyzed by the doped-metal catalysts, such as Pd/Al_2O_3[35], Ru[36], Au NPs[37], Ce/SiO_2[38], Cu[39], Fe/MOF[40], Co[41], and so on. However, for example, J. Yang[42] et al. had reported Au/TiO_2 nanospheres for oxidative coupling reactions of amines by visible-light, but the cycling test of the catalyst and the conversion to the product were not very good. Besides, the metal ion leaching of the catalyst in the reaction system has a great influence on the activity of the catalyst and the separation of the product. Furthermore, nitrile compounds also play a significant role in the field of pharmacological, functional organic chemistry and biological.[43] Typically, based on the earlier literature, synthesis amides, aldehydes and amines by controlling additives types for transfer hydrogenation of nitriles are considered an effective and green method.[43-47] However, though many excellent reaction systems regarding with transfer hydrogenation of nitriles have been reported, these processes mentioned above still required the metal species as activity sites to induce the reaction. Similarly, these metal supported

catalysts also had poor circulation and recyclability. Thus, it is highly desirable to develop a facile, green, efficient and sustainable method for the formation of imines and other chemical products. Herein, the highly efficient multifunctional NC nanosheets catalyst system for the synthesis of imines and transfer hydrogenation of nitriles under mild and controllable conditions was reported. The results confirmed that the catalyst for heterogeneous catalysis was synthesized successfully with a remarkably catalytic effect. Based on the application and characterization of the NC catalyst, graphitic-N was proved as the active sites which formed under its designated prepared temperature. The data obtained after repeated experiment showed that most of the yields of imines were more than 90 %. Cycling performance can be remained at least seven runs without reaction activity decay, which was comparable to the activity of those metal catalysts. Subsequently, the kinetic study was also carried out to testify the catalytic performances were rational. In a word, a green, highly-efficient and sustainable catalyst for resultant imines and transfer hydrogenation nitriles reaction were investigated, and it is beneficial to comprehend the mechanism of the metal-free N-doped carbon catalyst for resultant imines in this work.

2. Experimental

View Article Online
DOI: 10.1039/C9GC00908F

2.1. Reagents and chemicals

All reagents and chemicals were of analytical grade and used as received without any further purification. 3-Aminophenol (C_6H_7NO, 98%) was purchased from Shanghai McLean biochemical technology co., Ltd. Formaldehyde Solution (HCHO, 37%) was purchased from Tianjin Da Mao chemical reagents factory. Melamine ($C_3N_3(NH_2)_3$), Graphite powder and Potassium carbonate (K_2CO_3) were purchased from Sinopharm Chemical Reagents Co., Ltd.

2.2. Synthesis of the catalyst of porous N-doped carbon (NC)

For the synthesis of the porous N-doped carbon nanosheets, 3-Aminophenol, ethanol and deionized water were thoroughly dissolved in a 50 mL round-bottomed flask by ultrasound. Then, $NH_3 \cdot H_2O$ was dropwise added to the mixture, and it was dramatically stirred at 30 ˚C for 0.5 h. Subsequently, formalin (10 mL) was drop by drop added to the mixture, and the colloid was aged at 30 ˚C for 4 h. Sequentially, melamine and K_2CO_3 were added into the flask. After stirring for a further 0.5 h, a homogeneous precursor solution was obtained. The obtained solution was collected into a 50 mL stainless steel teflon autoclave and kept in an electric oven at 110 °C for 24 h. After cooling down naturally, the yellow precipitates were collected by filtration and followed by drying

View Article Online
DOI: 10.1039/C9GC00908F

in a vacuum oven at 60 °C for 12 h, and it was named as NC-110. Later, the dried precursor particles carbonized at a series of temperatures i.e. 500, 600, 700, 800, 900 ˚C for 120 min each, under Ar (8% H_2) atmosphere at a heating rate of 2 ˚C·min^{-1}. The carbonized particles were washed several times using deionized water in the

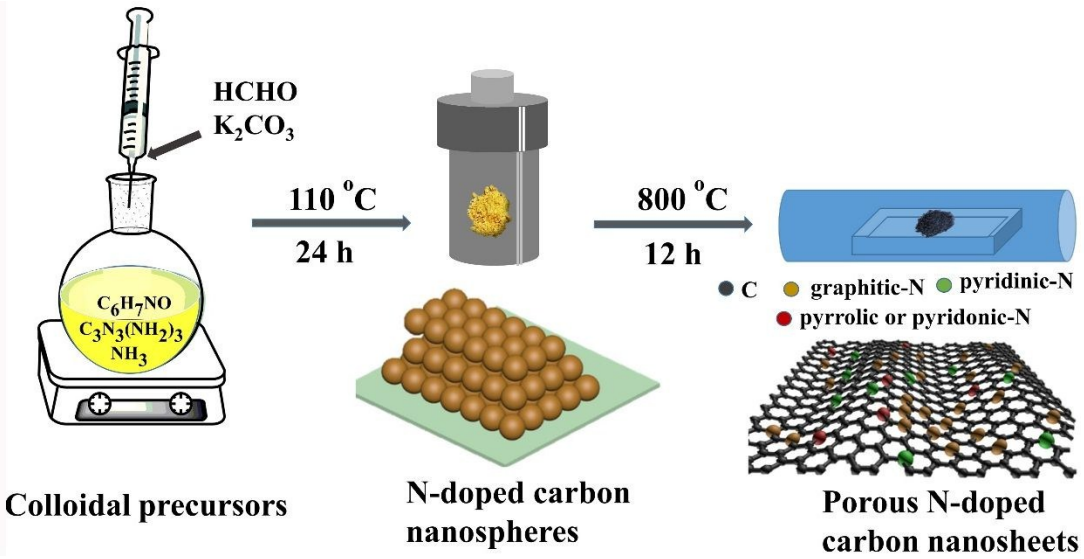

Scheme 1 The schematic caption of the synthesis of catalyst.

ultrasonic irradiation to promote the dissolve of K ions. Finally, the nanosheets particles were dried in a vacuum oven at 60 ˚C overnight. The materials were grinded to powder to get NC, named by NC-500, NC-600, NC-700, NC-800 and NC-900, severally. And all procedures remain unchanged, except for the amount of HCHO added only 5 mL, the catalysts were called NC-5-800 and NC-5-900. The schematic caption of the synthesis of catalyst was shown in Scheme 1.

2.3. Synthesis of the catalyst of N-doped graphite powder (GP-N)

Graphite powder (GP, 1.2 g) was washed several times by deionized water and dried in a vacuum oven at 60 ˚C overnight for reserved. Then, it was carbonized at 800 ˚C for 120 min under N_2 mixed with NH_3 atmosphere at a heating rate of 2 ˚C·min^{-1}. It was called GP-N-800.

2.4. Synthesis of the catalyst of g-C_3N_4

Melamine (1.2 g) was carbonized at 550 ˚C for 180 min under Ar atmosphere at a heating rate of 5 ˚C·min^{-1}. It was named for g-C_3N_4.

2.5. Catalytic conversion of imines

The reaction was tested in a 5 mL reaction tube with an air intake needle, oil bath, and thermocouple at atmospheric pressure. Typically, the NC-800 catalyst (15 mg), benzylamine (1 mmol), 1 mL dimethylsulfoxide (DMSO) and 0.5

View Article Online
DOI: 10.1039/C9GC00908F

mL deionized water (D: W=1:0.5) were mixed together and then magnetic stirring at 60 ˚C. The reaction time was 40 h and air was constantly taken into the tube by the air pump (10 mL·min^{-1}). The samples were extracted with deionized water and ethyl acetate after separation catalyst by centrifugation. The sample was analyzed by GC-MS (Agilent 6,890N/5,937N). Furthermore, the catalyst after reaction can be recycled and then it was washed with ethanol and deionized water several times, followed by a heat treatment (60 ˚C) before the next utilization.

2.6. Catalytic transfer hydrogenation of nitriles

Benzonitrile (1 mmol), NC-800 (20 mg) and additives were added into the 4 mL closed the high pressure reaction tube containing 1.5 mL mixed solvent (D: W=1:0.5) and then the reaction system stirred at 60 ˚C. After separated the catalyst and organic phase, the reaction resulting was analyzed by GC-MS.

2.7. Catalyst Characterization

In this study, these catalysts were in detail characterization to know its properties of physical and chemical, such as X-ray diffraction (XRD), the scanning electron microscopy (SEM) and transmission electron microscopy (TEM), nitrogen physisorption isotherms, X-ray photoelectron spectroscopy (XPS), fourier transform infrared spectroscopy (FT-IR), elemental analysis (EA), UV-Vis absorption spectra, and thermogravimetric analysis (TGA). The detail description of catalyst characterization instrument was in supporting information.

3. Result and discussion

3.1. Characterizations catalyst

To investigate the morphology and microstructures of a series of NC catalysts, the images were carried out by SEM and TEM. The SEM images of NC-110, NC-500, NC-600, NC-700, NC-800 and NC-900 were presented in Fig. 1 and Fig. S1. Fig. 1a indicated that the nanospheres could be uniformly formed at 110 ˚C. In Fig. S1, as the thermal decomposition temperature increased, the nanospheres were damaged and transformed into mesoporous nanosheets. And as shown in Fig. 1, it can be easily seen that more well-aligned in size distribution of mesoporous nanosheets were carbonized at 800 ˚C.

Meanwhile, two-dimensional mesoporous structure of NC-800 catalyst was proved by TEM image. From the TEM image of NC-800 in Fig. 2a, it can be seen that a mesoporous structure was successfully formed in the catalyst. The HRTEM image of NC-800 was shown in Fig. 2b. Besides, the HRTEM selected-area diffraction image (Fig. S2a) of NC-800 further revealed an amorphous carbon

View Article Online
DOI: 10.1039/C9GC00908F

Journal Name

ARTICLE

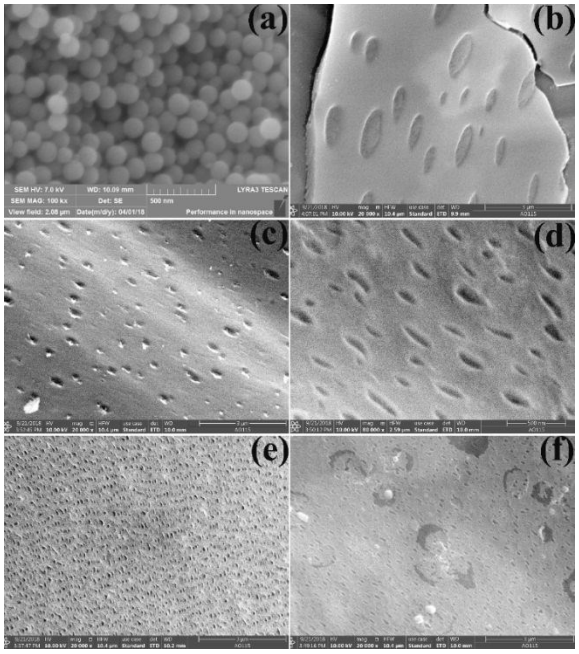

Fig. 1 SEM images of NC-110 (a), NC-500 (b), NC-600 (c), NC-700 (d), NC-800 (e) and NC-900 (f).

structure. In Fig. 2c, the high-angel annular dark field (HAADF) image of C and N element mappings demonstrated nitrogen was evenly doped in the carbon layer. In addition, the EDX of NC-800 was exhibited in Fig. S2.

The XRD pattern showed that NC was undefined structure, there were broad peak at around 25˚ (Fig. 3a), which corresponded to the (002) plane. Besides, for NC-700, NC-800 and NC-900, the other broad peak appeared at around 45˚, which indexed to the (100) plane. Meanwhile, with the carbonization temperature increases, the peaks intensity of NC became more and more stronger. At the same time,

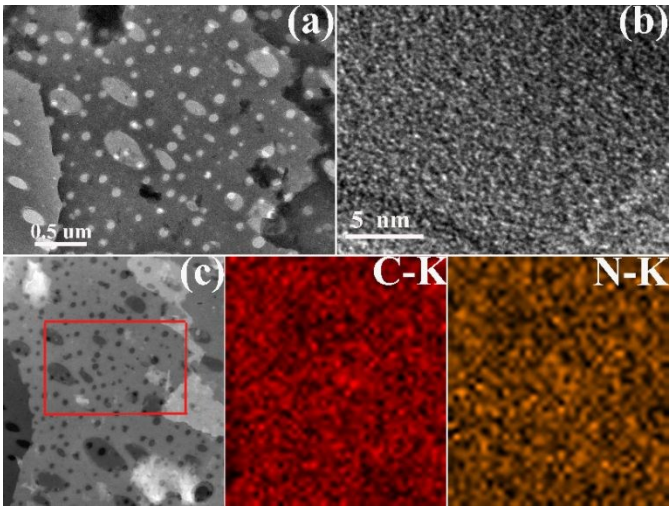

Fig. 2 TEM images of NC-800 (a), the HRTEM image showed amorphous carbon structure (b), and HAADF image (c) of C and N elements mapping images.

the XRD pattern of GP-CN-800 was exhibited in Fig. S3. Fig. 3b presented the Raman spectrum of NC, two distinct peaks around at 1380 and 1598 cm^{-1} indexed to D- and the G-bands, respectively. And the intensities of the D and the G bands demonstrated that a significant number of lattice defects existed in carbon framework due to N-doped. Moreover, with the temperature increased from 500 ˚C to 800 ˚C, the values of I_D/I_G increased from 0.958 to 1.015. In particular, when the temperature increased at 900 ˚C, the values dropped to 0.975. It could be concluded that the highest I_D/I_G value was attributed to NC-800, displaying its

View Article Online
DOI: 10.1039/C9GC00908F

structure owned the maximum concentration of defects.

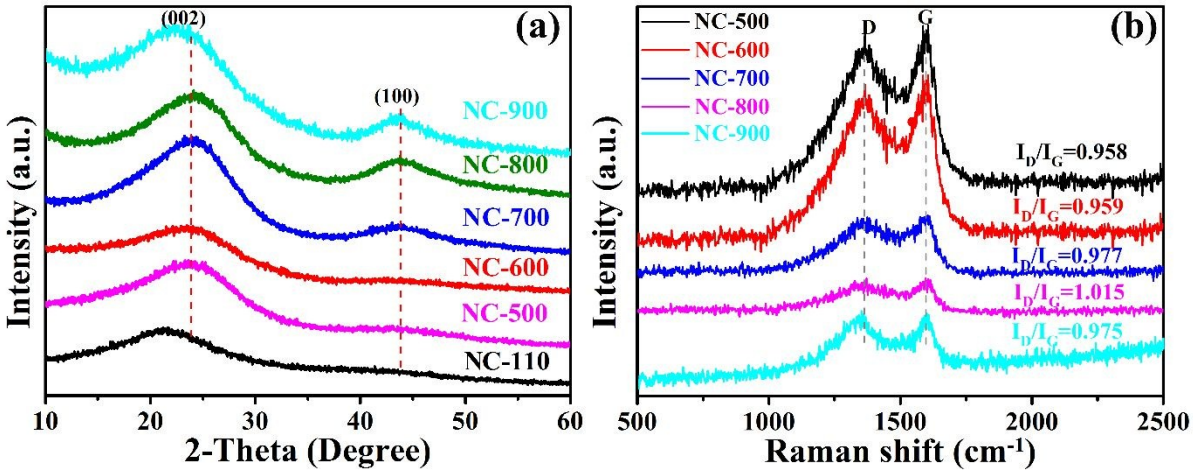

Fig. 3 XRD patterns (a) and Raman spectra (b) of the as-prepared NC catalysts.

The results of nitrogen adsorption-desorption isotherms for NC-500 to NC-900 were also shown in Table 1. Typically, the surface area of the catalyst obtained at higher carbonized temperature was larger than that at low temperature. In Table 1, it could be easily observed that the surface area of NC-800 catalyst is 594 m^2 g^{-1}, which slightly lower than NC-900 catalyst (638 m^2 g^{-1}) but farther higher than other catalyst. What's more, NC-800 catalyst showed type IV isotherms with a medium-pressure (P/P_0=0.47) and the high-pressure (P/P_0=1.0) region hysteresis loops, indicating that the catalyst mainly contains mesoporous structures with an average pore size of 0.28 nm in Fig. S4a.[48-51] However, for NC-900 catalyst, it mainly contained microporous structures with its nitrogen adsorption-desorption isotherms showed type I isotherms in Fig. S4b.

Table 1 Texture parameters of the series of prepared catalysts.

Samples	Surface area (m^2 g^{-1})	Average pore size (nm)	Pore volume (cm^3 g^{-1})
NC-500	6	57.8	0.01
NC-600	40	56.8	0.02
NC-700	91	11.0	0.04
NC-800	594	3.3	0.28
NC-900	638	3.2	0.34

FT-IR spectrogram was executed to farther elucidate the existed functional groups in catalysts from NC-110 to NC-900. In Fig. 4a, the peaks at 1200-500 cm^{-1} were assigned to C-C, C-N, C-O.

View Article Online
DOI: 10.1039/C9GC00908F

Especially, vibrational mode of 810-800 cm^{-1} was shown C-N heterocycles of triazine ring units.[52-54] The characteristic bands of 1700-1200 cm^{-1} are assigned to aromatic carbon and nitrogen heterocycles.[55, 56] Especially, the peaks at 1650-1550 cm^{-1} for the sp^2-hybridized C=C and C=N stretching region. [57-59] The primary bands in 3300-3500 cm^{-1} referred to the N-H stretching region.[60, 61] In addition, the band around 2934 cm^{-1} was contributed to C-H stretching vibrations, indicating both piperazine and triazine units existed in NC catalyst.[12, 25, 62] Furthermore, compared with 3-aminophenol and melamine in Fig. S5, the FT-IR spectrum of prepared catalysts indicated that these functional groups indeed existed. In addition, on account of the pyrolytic temperature increased, the characteristic bands of 850-750 cm^{-1} was disappeared. It may be due to the nanospheres consisted of triazine units cracked and derive the nanosheets. Fig. 4b illustrated the TG analysis (TGA) of NC-800, it could be obtained in the heated process with the N_2 atmosphere.

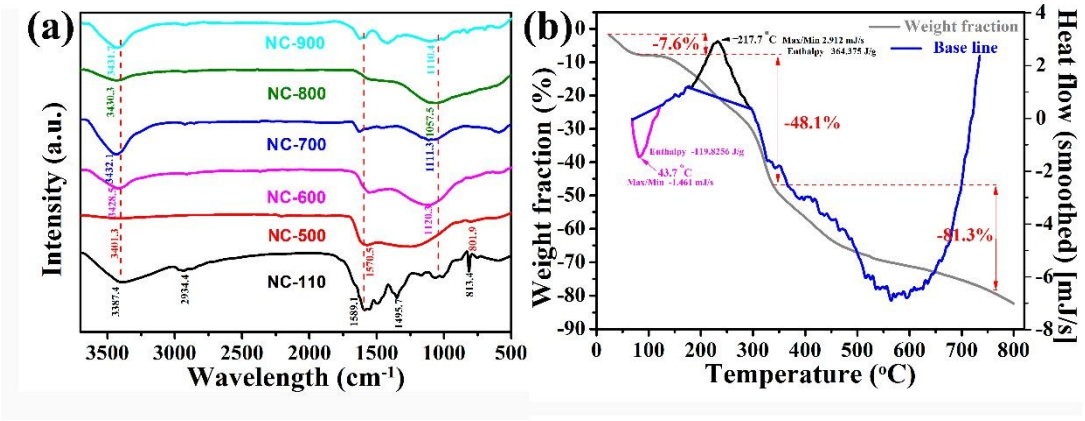

Fig. 4 FT-IR spectrogram of the as-prepared catalysts (a), TG+DSC curves measured in N_2 for NC-800 from 25 to 800 ˚C with a heating rate of 2 ˚C min^{-1} (b).

In the first stage of 25 to 150 ˚C, the catalyst showed the thermostability, and the 7.6% mass loss was due to the desorption of water in the polymer. There was a large weight fraction decreased about 40.5% in the region of 150 - 350 ˚C, which was ascribed to the pyrolysis of NC, and it could be concluded that the material completed the conversions of nanospheres to two-dimension nanosheets. In third stage, the weight loss achieved to 33.2% when it was heated to 800 ˚C. In combination with the SEM image, the mass loss is mainly caused by the thermal decomposition of

View Article Online
DOI: 10.1039/C9GC00908F

K_2CO_3 to form mesoporous, and further thermal decomposition of the nanosheets with some carbon and nitrogen functional groups lose in its structure. In addition, Fig. 4b also displayed the DSC curve for the thermal decomposition of the NC-800 catalyst from room temperature to 800 ˚C. The curve exhibited a rapid decomposition of the NC-800 with obvious endothermic peak at 217.7 ˚C and the exothermic peak at 43.7 ˚C. They were in good agreement with the data of NC material reported in the literature.[63, 64]

XPS was conducted to discuss the chemical elements binding states of C and N on the surface of NC and to investigate the probable reason of defect formation. The full-scan XPS spectrum of each NC catalyst contained C, N, and O elements was also exhibited in Fig. 5b and the contents of the elements was also listed in Table 2. The high-resolution spectrum of the C 1s in Fig. S6a could be divided into three peaks C-C (284.4 ± 0.2 eV), C-N (285.1 ± 0.2 eV) and C=N (286.1 ± 0.2 eV).[57, 65-68] The existence of C-N and C=N in the C 1s spectra was a strong evidence that N atoms successfully doped in the lattice of carbon. In Fig. 5a, besides NC-110, NC-800 and NC-900, the N 1s spectrum could be designated into three peaks, which were pyridinic-N (398.0 ± 0.2 eV), pyrrolic or pyridonic-N (399.00 ± 0.2 eV) and graphitic-N (400.3 ± 0.2 eV).[69] Especially, the N 1s spectrum of NC-110 catalyst only contained pyridinic-N and pyrrolic or pyridonic-N, and the N 1s spectrum of NC-800 catalyst only contained pyridinic-N and graphitic-N.[67, 68] As was said above, with the temperature increased from 500 ˚C to 800 ˚C (Table 2 and Fig. 5c), the tendency of contained graphitic-N was increased in matrix carbon, but pyridinic-N and

Table 2 The XPS analysis and element contents chemical analysis in the prepared catalysts.

Sample	XPS analysis				EA
	N (at. %)	Pyridinic-N (at. %)	Pyrrolic or pyrid--onic-N (at. %)	Graphitic-N (at. %)	N (wt. %)
NC-110	19.91	6.50	13.41	0	21.73
NC-500	10.44	5.54	3.05	1.85	17.08
NC-600	4.31	0.85	2.11	1.35	10.55

View Article Online
DOI: 10.1039/C9GC00908F

NC-700	4.11	0.58	0.89	2.64	8.31
NC-800	2.51	0.47	0	2.04	5.71
NC-900	1.44	0.61	0.49	0.34	0.86
NC-5-800	-	-	-	-	6.57
NC-5-900	-	-	-	-	1.85

pyrrolic or pyridonic-N decreased. It was accounted that graphitic-N could give rise to inhomogenous distribution of electrons in the π-system, enhanced the electron transfer throughout carbon plane, thus improved the activity and stability of catalyst.[49] However, when pyrolytic temperature reached to 900 ˚C, the contained graphitic-N in NC-900 catalyst was sharply dropped to 0.36 at. %, the contained pyrrolic or pyridonic-N increased. One reason was that the graphitic-N may be pyrolyzed at the high temperature, the other was that the pyridonic-N transformed into pyrrolic or pyridonic-N due to the hydrogen atmosphere under the high temperature carbonization conditions. Meanwhile, all of the NC catalysts tested by XPS wide-scan spectra exhibited the N contents had a declining trend when the calcination temperature increased. Similarly, the N contents of prepared NC catalysts detected by element contents chemical analysis showed the same trend. As for NC-5-800 and NC-5-900, the N contents were higher than the NC-800 and NC-900, respectively, which were determined by EA. Furthermore, the wide-scan XPS spectrum of GP-N-800 presented in Fig. S6b.

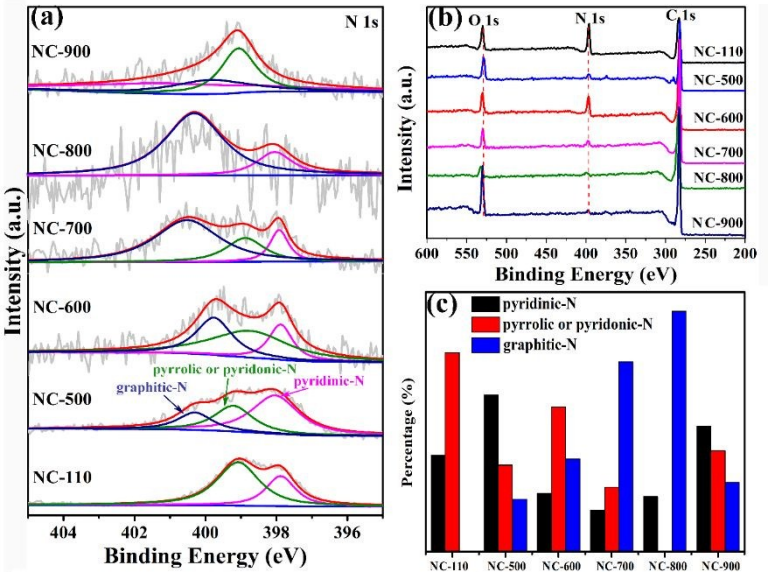

Fig. 5 High-resolution N 1s spectra (a), XPS wide-scan spectra (b), and the percentages of pyridinic-N, pyrrolic or pyridonic-N and graphitic-N of the NC catalysts (c).

View Article Online
DOI: 10.1039/C9GC00908F

Journal Name

ARTICLE

3.2. Catalyst performance

In order to present the catalytic activity and application, Table 3 showed comparison of the different catalysts. Obviously, the NC-800 was quite different with other catalysts in the self-oxidation of primary amines reaction under environmentally friendly condition. It could be easily seen from Table 3 when the temperature were at 60 and 120 ˚C (entries 1 and 4), the yields could reach to 99.9 % after reaction 40 and 8 h, respectively. For entries 1 and 4, when the reaction temperature at 60 °C, it is inconvenient to investigate the kinetic study of this reaction that the reaction took a long time to fully convert amine to imine. Therefore, by increasing the reaction temperature to calculate the activation energy of the reaction is needed. Meanwhile, compared entries 1-7 with entries 8-12 and 17-23, it could be explicitly observed that the NC-800 was superior to other catalysts, which was unquestionable in yield at the same reaction condition. According to the yields of entries 1-7, with the temperature increased from 50 to 130 ˚C, the NC-800 could effectually enhance the conversion rate of the reaction. Therefore, although the reaction temperature at 60 °C was considered to be a mild condition, it is a good choice to control the reaction conditions at 120 °C, which was advantageous for the reaction to obtain an effective conversion rate in a short time for substrate expansion and kinetic study. And there is no doubt that the reaction could also indeed occur at low temperatures though it needed long reaction time, such as at 50 and 70 ˚C. The entries 4 and 13-16 explained that the effect of catalyst amount to the reaction, which were demonstrated the optimal amount was 15 mg and the minimum catalyst amount was 5 mg. Because the turnover frequency (TOF) values of entry 4 surpassed the any other reaction conditions. But for entry 13, when the catalyst amount was 5 mg, it was shown the conversion of the reaction was only 13%. Selecting entries 17, 18, 20 and 23 for comparison, it was found that only graphene with a large BET surface area could catalyze the reaction, but the conversion was very low. Based on the results discussed above, it suggested that carbon atoms were not mainly active sites, and the catalyst should need a large BET surface area that the substrate would be absorbed on it. Notably, compared entry 18 with 19, it was undisputed that the conversion rate of the reaction increased due to the N-doped, which may illustrate nitrogen atoms were mainly active sites for this reaction. In short, with Table 3, it can be concluded that the yields of the reaction had greatly changed with the increased of graphite-N content. It was the strong evidence that nitrogen atoms, especially graphite-N, were

View Article Online
DOI: 10.1039/C9GC00908F

mainly active sites. In addition, it was unexpected that the NC-800 catalyst could be applied in transfer hydrogenation reaction of benzonitrile. For entries 8-11, it was initially discovered that as the reaction time prolonged, the sub-product of oxidative coupling of benzylamine gradually changed from benzonitrile to benzaldehyde.

Table 3 The catalytic activities of the different catalysts.[a]

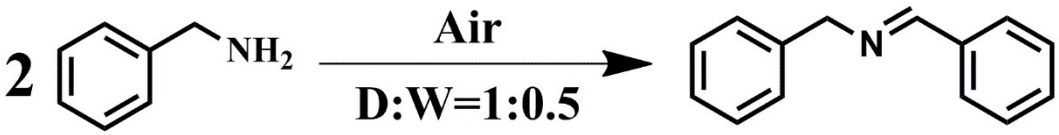

Entry	Catalyst/ (mg)	Temp. (˚C)	Time (h)	Conv./ Sel. (%)	TOF (mol·g^{-1} h^{-1})[b]
1	**NC-800/ 15**	**60**	**40**	**99.9/99.9**	**1.67×10^{-3}**
2	NC-800/ 15	50	40	73/99.9	1.22×10^{-3}
3	NC-800/ 15	70	40	99.9/99.9	1.67×10^{-3}
4	**NC-800/ 15**	**120**	**8**	**99.9/99.9**	**8.34×10^{-3}**
5	NC-800/ 15	130	8	99.9/65	1.67×10^{-3}
6	NC-800/ 15	110	8	89/99.9	7.42×10^{-3}
7	NC-800/ 15	100	8	82/99.9	6.83×10^{-3}
8	NC-900/ 15	120	8	40/79	3.34×10^{-3}
9	NC-700/ 15	120	8	90/85	7.50×10^{-3}
10	NC-600/ 15	120	8	83/78	6.92×10^{-3}
11	NC-500/ 15	120	8	48/80	4.00×10^{-3}
12	NC-110/ 15	120	10	-	-
13	NC-800/ 5	120	8	13/99.9	3.25×10^{-3}
14	NC-800/ 10	120	8	63/99.9	7.89×10^{-3}
15	NC-800/ 20	120	7	99.9/99.9	7.07×10^{-3}
16	NC-800/ 25	120	6.5	99.9/99.9	6.09×10^{-3}
17	Graphene/ 4	120	8	20/99.9	6.25×10^{-3}
18	GP-800/ 15	120	8	-	-
19	GP-N-800/ 15	120	8	17/99.9	1.42×10^{-3}
20	g-C_3N_4/ 15	120	8	25/85	2.08×10^{-3}
21	NC-5-800/ 15	120	8	99.9/97	8.34×10^{-3}
22	NC-5-900/ 15	120	8	47/80	3.92×10^{-3}
23	CNTs/ 15	120	8	-	-

Journal Name ARTICLE

24	none	120	8	-	-

View Article Online
DOI: 10.1039/C9GC00908F

[a] Reaction conditions: 1 mmol benzylamine, 15 mg catalyst, 1.5 mL solvent (D:W=1:0.5) and air was brought in reaction system by pump with 10 mL/min. The conversion and selectivity were detected by GC-MS. [b] Turnover frequency (TOF) = mol of benzylamine converted per gram of catalyst per hour.

As is well known, the solvent with higher polarity is more beneficial to the conversion of benzylamine. Therefore, it was found that D:W= 1:0.5 was the best one among the solvents tested (Table 4, entries 7, 15) as compare to common solvents, such as N, N-dimethyl-formamide (DMF), CH_3CN, toluene, DMSO and so on.[70] Especially, for entry 10, though the TOF value of the reaction surpassed any other reaction conditions, its yield of the reaction was not higher than entries 7 and 15. However, the catalytic activity of the catalysts is due to doped carbon itself and not due to potential contamination with traces of metal ions is not absolutely clear. In view of this, we designed a comparative experiment in which metal ions (such as KCl and NaCl) that may remain in the nitrogen-doped carbon catalyst were added under the same reaction conditions. It is easy to find that the conversion of the product is trace. Then, we simultaneously added NC-800 catalyst and KCl (or NaCl) and tested under the same reaction conditions. The results showed a slight decrease in the selectivity of the product. Therefore, we can draw a rough conclusion that the mainly catalytic activity is due to the doping of nitrogen on carbon, and the more impurity metal ions contained in the target catalyst, the weaker the catalytic activity. Detailed data of the comparative experiment was shown in supporting information (Table S1).

Table 4 The catalytic activities of NC-800 in the different solvents.[a]

Entry	Temp. (°C)	Time (h)	Solvent/ 1.5 mL	Conv. (%)	Yield (%)	TOF ($mol \cdot g^{-1} h^{-1}$)
1	60	40	CH_3CN	80	80	1.34×10^{-3}
2	60	40	Toluene	86	86	1.44×10^{-3}

View Article Online
DOI: 10.1039/C9GC00908F

3	60	40	Water	-	-	-
4	60	40	Ethanol	20	20	0.34×10^{-3}
5	60	40	DMSO	94	94	1.57×10^{-3}
6	60	40	1, 4-dioxane	72	72	1.20×10^{-3}
7	**60**	**40**	**D:W =1:0.5**	**99.9**	**99.9**	**1.65×10^{-3}**
8	120	8	DMSO	99.9	70	8.34×10^{-3}
9	120	8	DMF	96	63	8.00×10^{-3}
10[b]	**120**	**24**	**Solvent-free**	**99.9**	**80**	**13.86×10^{-3}**
11	120	8	D:W =1.4:0.1	99.9	68	8.34×10^{-3}
12	120	8	D:W =1.3:0.2	99.9	75	8.34×10^{-3}
13	120	8	D:W =1.2:0.3	99.9	82	8.34×10^{-3}
14	120	8	D:W =1.1:0.4	99.9	94	8.34×10^{-3}
15	**120**	**8**	**D:W =1:0.5**	**99.9**	**99.9**	**8.34×10^{-3}**
16	120	8	D:W=0.9:0.6	60	60	5.00×10^{-3}
17[c]	120	8	Water	52	52	4.34×10^{-3}
18[d]	120	8	Water	5	5	0.42×10^{-3}

[a] Reaction conditions: 1 mmol benzylamine, 15 mg NC-800 catalyst and air was brought in reaction system by pump with 10 mL/min. The conversion and selectivity were detected by GC-MS. [b] 5 mmol benzylamine. [c] 1 mmol benzylamine, 15 mg NC-800 catalyst and the filled with O_2 reacted at the closed the high pressure reaction tube. [d] 1 mmol benzylamine, 15 mg NC-800 catalyst and the filled with N_2 reacted in the closed the high pressure reaction tube.

Moreover, to explore the wide applicability of the NC-800 catalyst, other types of amines, cyanides and nitriles were all used for the substrate extension reaction under the optimal reaction condition, severally. Each type substrate was converted to relevant product with high yield shown in Table 5 and Table 6. In Table 5, the reactions of converted imines by various amines had high yields. Meanwhile, for entries 1-16, it could be induced that as the ability of the electron donating group was weakened, the yield of the imine was improved under the optimum reaction conditions. That is to say, NC-800 is more suitable for the oxidative coupling reaction of benzylamine derivatives having an electron withdrawing group. As for entries 17-24 in Table 5, when two amines with a molar ratio of 1:1 were added to the reaction system, the highest yields could reach 64 %. In addition, for the reaction of the oxidation of amines, when we performed NC-600, NC-700 or NC-900 to react, it was found that the presence of benzaldehyde and benzonitrile was present in the detection of the product. And the concentration of benzaldehyde present in the sub-product is higher than that of benzonitrile with the reaction time increasing. Therefore, in Table 6, the high yields

View Article Online
DOI: 10.1039/C9GC00908F

for catalytic transfer hydrogenation of nitriles were also confirmed the outstanding catalytic performance of NC-800 at the low temperature. Adding different additives, the final products of these reactions were totally different, we could obtain aldehydes, amides, and amines by adding K_2CO_3, KOH, and $NaBH_4$, respectively. Finally, in Table S2, when only adding additives, the comparative experiments also exhibited that the effect of the transfer hydrogenation of nitriles reaction system was extremely declined without NC-800 catalyst. By consulting a large amount of literature, for the reaction of nitrile to aldehyde, the reducing agent is H_2O. In addition, we add K_2CO_3 into the reaction of nitrile to aldehyde to provide a weak alkaline environment and the mechanism of the reaction were also shown in Scheme 2. Furthermore, as is well known, the transformation of nitrile to carboxamide is hydrolysis reaction. From the comparative experiment in Table S2, the results demonstrated that the reaction yield is almost 30% without the addition of NC-800 and only adding KOH. When NC-800 and KOH are added at the same time in the reaction, the yield of the product reaches the maximum under the same reaction conditions. In view of this, we believe that the hydrolysis reaction occurs due to the simultaneous presence of KOH and NC-800 in the reaction, which play a synergistic role. And for the reduction of nitrile to amine, the reducing agent is $NaBH_4$. Its mechanism of action is the nucleophilic addition of H to the positive charge center by the dissociation of $NaBH_4$. And NC-800 catalyst makes the process of nucleophilic addition easier. All in all, for the transfer hydrogenation of nitriles reaction, the reaction scope was most aromatic nitriles and some fatty cyanides. Meanwhile, from Table S3, it was found that the catalytic performance of the metal-free nitrogen-doped carbon catalyst can be comparable to that of the metal-supported catalysts through experimental tests.

Table 5 The imines reaction of various amines by NC-800.

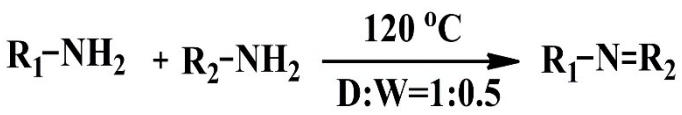

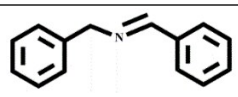
(1)[a] Y [c]: 99.9 % (8 h)

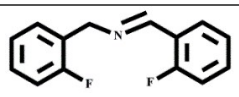
(2)[a] Y: 99.9 % (8 h)

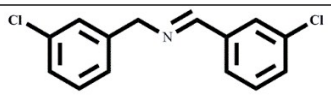
(3)[a] Y: 80.5 % (8 h)

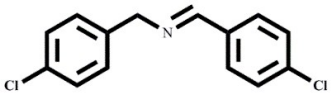
(4)[a] Y: 96.0 % (9 h)

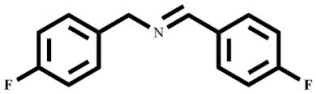
(5)[a] Y: 97.0 % (9 h)

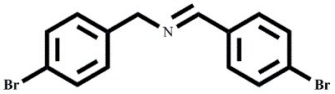
(6)[a] Y: 80.9 % (9 h)

View Article Online
DOI: 10.1039/C9GC00908F

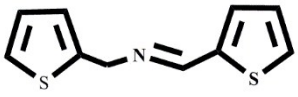

(7)[a] Y: 91.0 % (10 h)

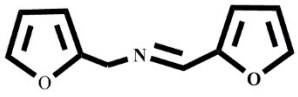

(8)[a] Y: 99.9 % (10 h)

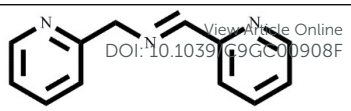

(9)[a] Y: 99.9 % (8 h)

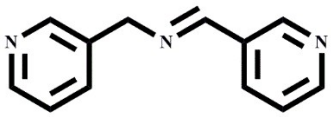

(10)[a] Y: 93.0 % (8 h)

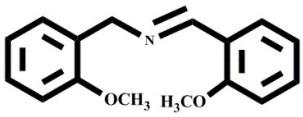

(11)[a] Y: 65 % (10 h)

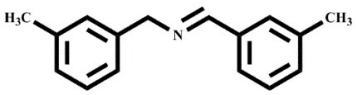

(12)[a] Y: 92.0 % (8 h)

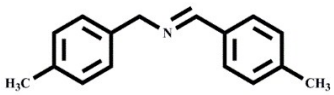

(13)[a] Y: 81.0 % (8 h)

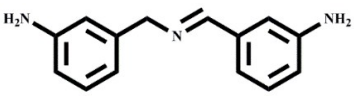

(14)[a] Y: 29.0 % (10 h)

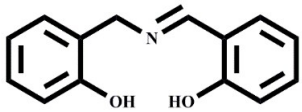

(15)[a] Y: 45.5 % (8 h)

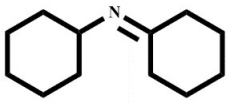

(16)[b] Y: 56.0 % (12 h)

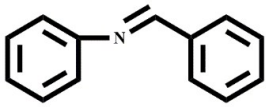

(17)[a] Y: 99.9% (10 h)

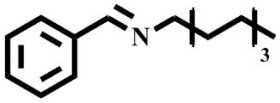

(18)[a] Y: 49.0 % (10 h)

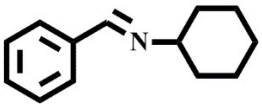

(19)[b,] Y: 56.8% (12 h)

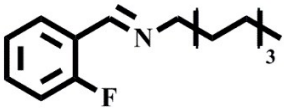

(20)[a] Y: 64.0 % (10 h)

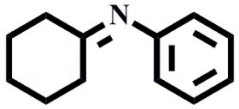

(21)[b] Y: 30.0 % (12 h)

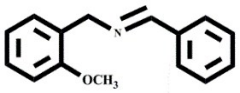

(22)[a] Y: 45.0 % (10 h)

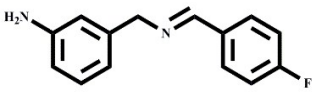

(23)[a] Y: 20.0 % (10 h)

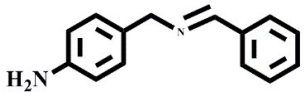

(24)[a] Y: 27.0 % (10 h)

[a] Reaction conditions: 1 mmol amines, 15 mg NC-800 catalyst 1.5 mL solvent (D:W=1:0.5) and air was brought in reaction system by pump with 10 mL/min. The conversion and selectivity were detected by GC-MS. [b] 1 mmol amines, 15 mg NC-800 catalyst, 1.5 mL solvent (D:W=1:0.5) and the filled with O_2 reacted in the closed the high pressure reaction tube. [c] Y= yield (%).

Table 6 The transfer hydrogenation of nitriles.

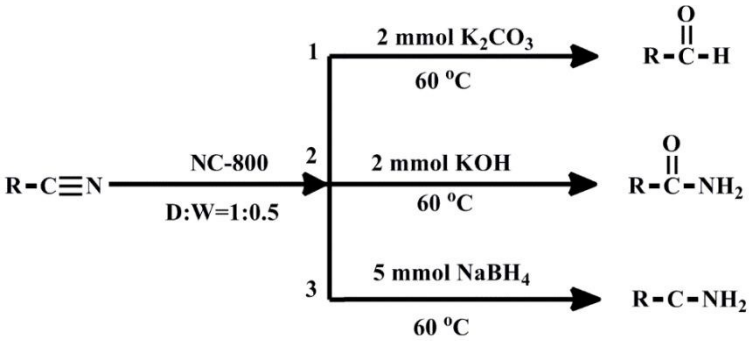

1	2	3

View Article Online
DOI: 10.1039/C9GC00908F

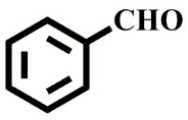	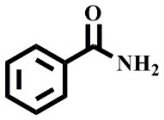	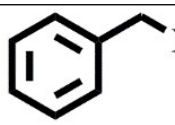
1.(1)[a] Y: 99.9 % (8 h)	2.(1)[b] Y: 99.9 % (8 h)	3.(1)[c] Y: 99.9 % (6 h)
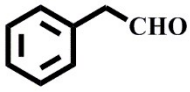	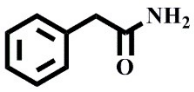	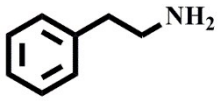
1.(2)[a] Y: 60.0 % (10 h)	2.(2)[b] Y: 87.0 % (8 h)	3.(2)[c] Y: 99.9 % (6 h)
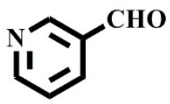	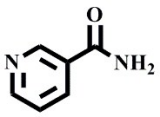	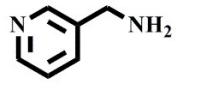
1.(3)[a] Y: 99.9 % (8 h)	2.(3)[b] Y: 99.9 % (8 h)	3.(3)[c] Y: 99.9 % (6 h)
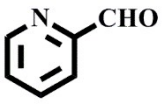	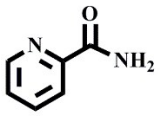	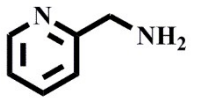
1.(4)[a] Y: 99.9 % (8 h)	2.(4)[b] Y: 99.9 % (8 h)	3.(4)[c] Y: 99.9 % (6 h)
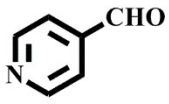	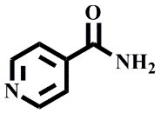	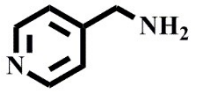
1.(5)[a] Y: 99.9 % (8 h)	2.(5)[b] Y: 99.9 % (8 h)	3.(5)[c] Y: 99.9 % (6 h)
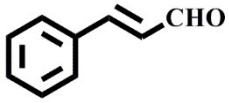	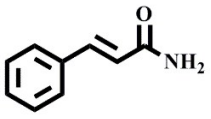	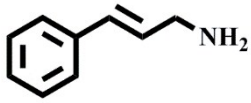
1.(6)[a] Y: 99.9 % (6 h)	2.(6)[b] Y: 99.9 % (8 h)	3.(6)[c] Y: 99.9 % (6 h)
		
1.(7)[a] Y: 99.9 % (8 h)	2.(7)[b] Y: 99.9 % (8 h)	3.(7)[c] Y: 99.9 % (4.5 h)
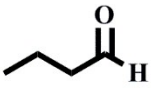	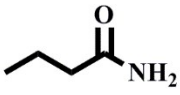	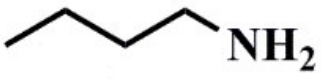
1.(8)[a] Y: 99.9 % (8 h)	2.(8)[b] Y: 99.9 % (8 h)	3.(8)[c] Y: 99.9 % (4.5 h)

[a, b, c] Reaction conditions: 1 mmol nitriles, 20 mg NC-800 catalyst and 1.5 mL solvent (D:W=1:0.5) reacted in the closed the high pressure reaction tube at 60℃. The conversion and selectivity were detected by GC-MS.

[a] Extra adding 2 mmol K_2CO_3, [b] extra adding 2 mmol KOH, and [c] extra adding 5 mmol $NaBH_4$.

View Article Online
DOI: 10.1039/C9GC00908F

Journal Name

ARTICLE

3.3. Kinetic study

To realize the mechanism and the order of the reaction of the imines reaction, the kinetic study of the reaction was explored. The overall kinetics equation of the reaction could be defined as:

$$[\text{Amine}] + [\text{O2}] \xrightarrow{K} [\text{Imine}] + \text{NH3} + \text{H2O} \quad (1)$$

The formulation of the reaction rate was given by Eq. (2). Where the $[C_A]$ represented the benzylamine, k represented the rate constant and the n_1, n_2 and n were the series of the [Cat.], $[O_2]$ and $[C_A]$, severally. Where the $[C_A]$, $[O_2]$ and [Cat.] were the concentration of substrate, oxygen and catalyst. Meanwhile, as previous assumed $[O_2]$ as a constant and combined the reported mechanism, the kinetic rate equation was derived with the constant K defined as: $K = k\,[\text{Cat.}]^{n^1}[O_2]^{n^2}$. Therefore, the Eq. (2) could be predigested to Eq. (3), and the equation of the reaction rate was given by Eq. (4-5). The K was the apparent rate constant of reaction, A was the pre-exponential factor, E_a was the activation energy, R was ideal gas constant (8.314 $J \cdot mol^{-1} \cdot K^{-1}$) and the T was the reaction temperature. In Fig. 6, in order to compute the n and E_a of the reaction, the specific concentration of benzylamine was calculated from 90 to 120 ˚C for different reaction time with the Eq. (2-5). It could be obviously calculated the total order was n = 0.314, and E_a was 67.39 kJ/mol. The apparent activation value is 67.39 kJ/mol (Fig. 6c), which is very similar to the reported value of 62.8 kJ/mol.[71] And the reported responses are assumed to be pseudo first-order reaction, but after we investigated, it was found that the order of the reaction is 0.314 in the work. Simultaneously, UV-Vis was also performed to analysis the reaction rate of the reaction in Fig. S7.

$$r = k[\text{Cat.}]^{n^1}[O_2]^{n^2}[C_A]^n \quad (2)$$

$$r = K[C_A]^n \quad (3)$$

$$K = Ae^{-E_a/RT} \quad (4)$$

View Article Online
DOI: 10.1039/C9GC00908F

$$lnK = lnA - \frac{E_a}{RT} \quad (5)$$

3.4 Catalyst recycled

Furthermore, the number of cycles of the catalyst was an important indicator of whether it could be industrialized. In view of this, the NC-800 catalyst could be easily separated from reaction system by centrifugation and then washed with ethanol and deionized water for three times, respectively. Then, the catalyst was dried in a vacuum oven at 60 ˚C for 12 h to farther assess the repeatability of the catalyst for the oxidation amines reaction. In Fig. 7, it was found that the yield of imine exceeded 99.9% after seven cycles experiment, indicating that the reusability and activity of the catalyst were very brilliant. The FT-IR and XPS of reused catalyst were shown in Fig. S8 and S10. The FT-IR spectrum demonstrated that the spectrum of reused catalyst was the same as the fresh, it proved that the catalyst was not damaged after cyclic test. And in Fig. S10, we can easily obtain that the binding energy of C 1s and N 1s have slight deviation in XPS spectrum. The possible factors are: the error of the experimental instrument or the electron transfer between the nitrogen-doped carbon material and the reaction substrate, so that the binding energy between the bonds on the material is slightly reduced. However, from the N 1s spectrum, the active sites was not destroyed and remained graphite-N.

3.5 Mechanism study

Distinctly, in order to investigate the mechanism of resultant imines reaction, the defect of two-dimensional NC nanosheets should be firstly studied. In Fig. 3b, as the calcination temperature increased, the values of I_D/I_G became larger, and it can be deduced that the defect carbon concentration in NC-500, NC-600, NC-700 and NC-800 increased in turn, which proved the high concentration of defective carbon could be ascribed to N-doped in the lattice of carbon. However, for NC-900, combined the EA (the content of N) values with the decreased value of I_D/I_G also demonstrated the formation of defect carbon due to the N doping. In addition, based on the analysis of XPS spectra of N 1s (Table 2 and Fig. 5), the N contents of NC catalysts also displayed the decreased tendency as the carbonized temperature increased from 500 ˚C to 900 ˚C, the EA showed the same trend as well. Moreover, the high-resolution

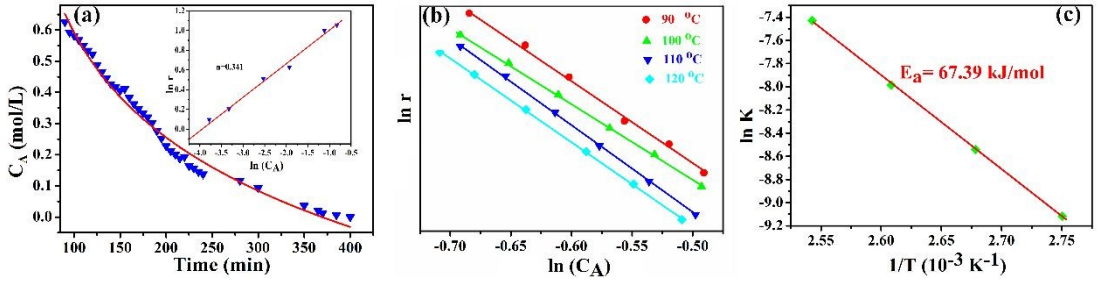

View Article Online
DOI: 10.1039/C9GC00908F

Fig. 6 The kinetic curve of the catalytic oxidation benzylamine (inset: the total order of the reaction) (a), the different reaction time at the different reaction temperature (b), and the reaction of activation energy (c).

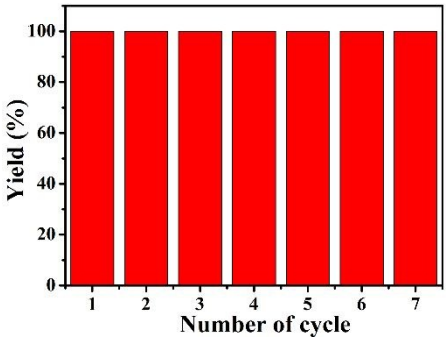

Fig. 7 The recyclability of the catalyst. (Reaction conditions: 15 mg NC-800 catalyst, 1 mmol benzylamine, 1.5 mL solvent (D: W=1:0.5) and air was brought in reaction system by pump with 10 mL/min at 120 ˚C for 8 h. The conversion and selectivity were detected by GC-MS.)

N 1s spectra could exhibited the content of graphitic-N in the NC material, which presented an increased trend in Fig. 5c. It might be given a clue that graphitic-N was the main cause of defects formation and the graphitic-N was the mainly active sites. Furthermore, in Fig. S8, FT-IR spectra proved that benzylamine was firstly absorbed in the catalyst, then to occur oxidation reaction. And it could be easily observed that at around 1425 cm^{-1} a new peak occurred. Meanwhile, the catalyst for the adsorption of benzylamine were also performed XPS full-scan spectra (Fig. S9) and the high-resolution spectrum of C 1s and N 1s (Fig. 8) analysis. Compared with the high resolution spectrum of N 1 s (Fig. 8b) of NC-800, it could be found that two new peaks occurred due to the adsorption of the substrate, one was attributed to the bond -NH_2 of benzylamine and the other was assigned to the new bond of graphitic-N and -NH2 group.[72] From Fig. 8, it could conclude that when compared NC-800 adsorbed benzylamine with NC-800, the binding energy had a significant shift toward the low binding energy, which was attributed to the interaction of lone pair electrons of N atom in NC-800 and the π electrons of benzylamine. It could be deduced that the transfer of electrons from benzylamine to NC-800 increased the charge density of NC-800, which leaded the reaction rapidly proceeding. In addition, the experimental

View Article Online
DOI: 10.1039/C9GC00908F

Journal Name

ARTICLE

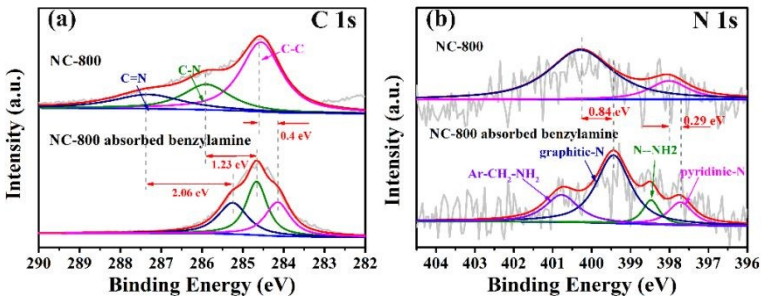

Fig. 8 Comparison of high resolution C 1s spectra (a), and N 1s spectra (b) between NC-800 and NC-800 adsorbed benzylamin.

results of this work (Table 3) also demonstrated the graphitic-N was the mainly active sites, and the high yields of imines could obtain when the graphitic-N existed. And when the reaction was not occurred at the optimal condition, a certain amount of benzaldehyde and benznitrile was detected in the product by GC-MS. It maybe present the path of oxidative dehydrogenation of primary amines.And it was also proved that the oxygen played a vitally crucial role in the reaction (entries 17 and 18). Meanwhile, butylated hydroxytoluene (BHT) was added to the reaction system to quench the synthesis of imines.[37, 73] The result was that large quantities benzaldehyde and imine were produced in the reaction. Moreover, other related carbon catalysts for this reaction play a key role in understanding this working mechanism. Previous research conjectured benzaldimine as an intermediate in the reaction of benzylamine to benzylimine.[74] However, it is difficult to prove the existence through the analysis method such as GC-MS. For example, Jones et al. proposed the same mechanism but the intermediate still did not have experimental proof to demonstrate.[75] Zhang et al. attempted to detect the intermediate by in situ NMR technique, but they also did not directly detect it at the end.[71] However, they thought that dibenzylamine and N-methyl-1-phenylmethanamine majorly generated the corresponding benzaldimines as detected by GC was indirectly proved the benzaldimine was intermediate in the reaction.[71]

Hence, based upon the above study and the previous reported literature (Table S3), the mechanism of the reaction should be legitimately proposed in Scheme 2. Generally, the primary amines reacted into imines involved two different oxidative dehydrogenation routes (Scheme 2, paths 1 and 2).[16, 35-38, 76, 77] Therefore, the reaction mechanism of the catalytic system was also no

View Article Online
DOI: 10.1039/C9GC00908F

exception. Nevertheless, the formation of RCH=NH as an intermediate from primary amines by NC-800 was common in the both steps. Firstly, amine and O_2 were activated by the catalyst to form active species, respectively, under the optimized reaction conditions. Then, in path 1, the formed imine intermediate was hydrolyzed imine to obtain aldehyde. After that, the aldehyde reacted with another amine molecule to form the targeted product. However, for path 2, the formed RCH=NH intermediate directly reacted with another amine molecule to obtain an aminal. Finally, the aminal missed a molecule of NH_3 to form the targeted compound. Meanwhile, as is well known, when the catalyst is added to the reaction, the reaction pathway will change. And when investigating the effect of the presence of the catalyst on the reaction, it was found that the reaction did not occur without the addition of the catalyst. Therefore, through the kinetic study of the reaction, we calculated the apparent activation value is 67.39 kJ/mol, which is very similar to the reported value of 62.8 kJ/mol.[71] Combined the reported literature with the above experimental results, the self-oxidative coupling of amines was mainly carried out through the path 1 in this work.

4. Conclusion

In this work, an environmentally friendly and multifunctional catalyst of two-dimensional mesoporous N-doped carbon for the oxidative resultant imines and transfer hydrogenation of nitriles had been investigated. Under an economically feasible reaction conditions such as air atmosphere, low temperature (60 ˚C) and low catalyst

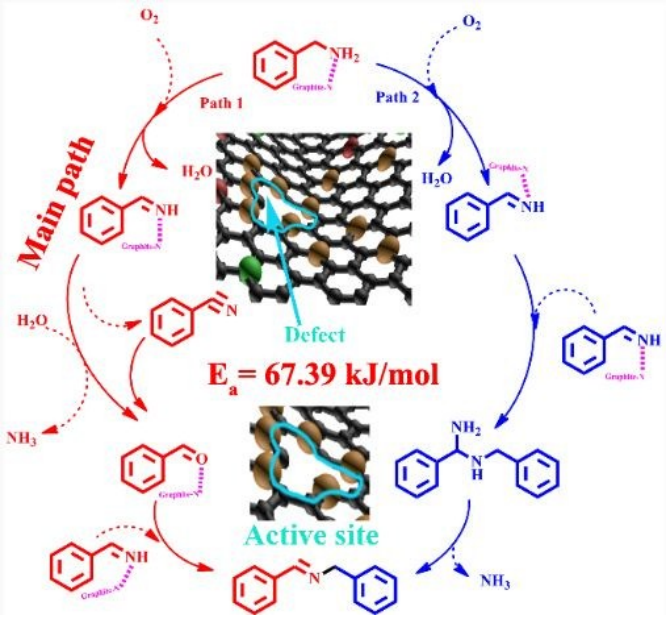

Scheme 2 Proposed mechanism of the reaction.

amount (15 mg), the NC-800 owned reputably catalytic performance, and a wide substrate scope for amines and nitriles transformed to the corresponding products. And the results showed that most of the yields of these four reactions were all over 90 %. According to excellently experimental results and the characterizations of the catalyst, we can conclude the nitrogen-doped carbon was formed defects in the catalysts are very important to the catalytic activity. In particular, graphite-N is considered to be the main active site in the catalyst. Moreover, the reaction of amine to imine on NC-800 does not follow the reported pseudo-first-order kinetics, which order is 0.314 and the apparent activation value is 67.39 kJ/mol. Particularly, the NC-800 had highly-stable catalytic performance and could be reused at least 7 times,

which show greatly potential performance in large-scale production. In summary, the simple preparation and outstanding activity of the catalyst would offer a valid way to the sustainable green chemistry.

Conflicts of interest

There are no conflicts to declare.

References

1. D. Pech, M. Brunet, H. Durou, P. Huang, V. Mochalin, Y. Gogotsi, P.-L. Taberna and P. Simon, *Nat. Nanotechnol.*, 2010, **5**, 651.
2. C. Peng, X.-b. Yan, R.-t. Wang, J.-w. Lang, Y.-j. Ou and Q.-j. Xue, *Electrochim. Acta*, 2013, **87**, 401-408.
3. J. Ma, Y. Ma and F. Yu, *ACS Sustain. Chem. Eng.*, 2018, **6**, 8178-8191.
4. S. Zhao, C. Zhao, X. Li, F. Li, L. Jiao, W. Gao and R. Li, *RSC Adv.*, 2016, **6**, 76582-76589.
5. Z. Daşdelen, Y. Yıldız, S. Eriş and F. Şen, *Appl. Catal. B-Environ.*, 2017, **219**, 511-516.
6. Q. Wang, H. Liu, R. Li, M. Yang, Z.-B. Wang, L. Zhang, C. Li and D.-M. Gu, *ACS Appl. Mater. Inter.*, 2017, **9**, 44512-44518.
7. D.-W. Wang, F. Li, Z.-G. Chen, G. Q. Lu and H.-M. Cheng, *Chem. Mater.*, 2008, **20**, 7195-7200.
8. Y. Lin, S. Wu, W. Shi, B. Zhang, J. Wang, Y. A. Kim, M. Endo and D. S. Su, *Chem. Commun.*, 2015, **51**, 13086-13089.
9. J. Tong, Q. Li, W. Li, W. Wang, W. Ma, B. Su and L. Bo, *ACS Sustain. Chem. Eng.*, 2017, **5**, 10240-10247.
10. Y. Song, W. Chen, C. Zhao, S. Li, W. Wei and Y. Sun, *Angew. Chem. Int. Ed.*, 2017, **56**, 10840-10844.
11. C. Ruiz-García, F. Heras, L. Calvo, N. Alonso-Morales, J. J. Rodriguez and M. A. Gilarranz, *Appl. Catal. B-Environ.*, 2018, **238**, 609-617.
12. Y. Leng, J. Li, C. Zhang, P. Jiang, Y. Li, Y. Jiang and S. Du, *J. Mater. Chem. A*, 2017, **5**, 17580-17588.
13. Y. Sun, I. Sinev, W. Ju, A. Bergmann, S. Dresp, S. Kühl, C. Spöri, H. Schmies, H. Wang, D. Bernsmeier, B. Paul, R. Schmack, R. Kraehnert, B. Roldan Cuenya and P. Strasser, *ACS Catal.*, 2018, **8**, 2844-2856.
14. J.-Y. Park, D.-H. Kwak, K.-B. Ma, S.-B. Han, G. S. Chai, S.-K. Kim, D.-H. Peck, C.-S. Kim, A. Kucernak and K.-W. Park, *J. Catal.*, 2018, **359**, 46-54.
15. W. Chen, J. Shi, T. Zhu, Q. Wang, J. Qiao and J. Zhang, *Electrochim. Acta*, 2015, **177**, 327-334.
16. J. Ye, K. Ni, J. Liu, G. Chen, M. Ikram and Y. Zhu, *ChemCatChem*, 2018, **10**, 259-265.
17. M. Algarra, D. Bartolić, K. Radotić, D. Mutavdžić, M. S. Pino-González, E. Rodríguez-Castellón, J. M. Lázaro-Martínez, J. J. Guerrero-González, J. C. G. Esteves da Silva and J. Jiménez-Jiménez, *Talanta*, 2019, **194**, 150-157.
18. Y. Wen, B. Wang, C. Huang, L. Wang and D. Hulicova-Jurcakova, *Chem.-Eur. J.*, 2015, **21**, 80-85.
19. J. R. Maluta, S. A. S. Machado, U. Chaudhary, J. S. Manzano, L. T. Kubota and I. I. Slowing, *Sens. Actuators B Chem.*, 2018, **257**, 347-353.
20. W. Wu, Q. Zhang, X. Wang, C. Han, X. Shao, Y. Wang, J. Liu, Z. Li, X. Lu and M. Wu, *ACS Catal.*, 2017, **7**, 7267-7273.
21. L. Miao, D. Zhu, M. Liu, H. Duan, Z. Wang, Y. Lv, W. Xiong, Q. Zhu, L. Li, X. Chai and L. Gan, *Chem. Eng. J.*, 2018, **347**, 233-242.
22. M. Latorre-Sánchez, A. Primo and H. García, *Angew. Chem. Int. Ed.*, 2013, **52**, 11813-11816.
23. C. Schäfer, C. J. Ellstrom, H. Cho and B. Török, *Green Chem.*, 2017, **19**, 1230-1234.
24. Y. Yang, C.-J. Sun, D. E. Brown, L. Zhang, F. Yang, H. Zhao, Y. Wang, X. Ma, X. Zhang and Y. Ren, *Green Chem.*, 2016, **18**, 3558-3566.
25. N. D. Shcherban, P. Mäki-Arvela, A. Aho, S. A. Sergiienko, P. S. Yaremov, K. Eränen and D. Y. Murzin, *Catal. Sci. Technol.*, 2018, **8**, 2928-2937.
26. X.-k. Kong, Z.-y. Sun, M. Chen, C.-l. Chen and Q.-w. Chen, *Energy Environ. Sci.*, 2013, **6**, 3260-3266.
27. M. Li, F. Xu, H. Li and Y. Wang, *Catal. Sci. Technol.*, 2016, **6**, 3670-3693.
28. B. Chen, L. Wang, W. Dai, S. Shang, Y. Lv and S. Gao, *ACS Catal.*, 2015, **5**, 2788-2794.
29. S. Furukawa, R. Suzuki and T. Komatsu, *ACS Catal.*, 2016, **6**, 5946-5953.
30. V. V. Patil, E. M. Gayakwad and G. S. Shankarling, *J. Org. Chem.*, 2016, **81**, 781-786.
31. D. P. Narayanan, S. K. Cherikallinmel, S. Sankaran and B. N. Narayanan, *J. Colloid Interf. Sci.*, 2018, **520**, 70-80.
32. B. Majumdar, D. Sarma, S. Jain and T. K. Sarma, *ACS Omega*, 2018, **3**, 13711-13719.
33. R. Ramesh, G. Sankar, J. G. Malecki and A. Lalitha, *J. Iran. Chem. Soc.*, 2018, **15**, 1-9.
34. A. Fernandes and B. Royo, *ChemCatChem*, 2017, **9**, 3912-3917.
35. V. S. Marakatti, S. C. Sarma, B. Joseph, D. Banerjee and S. C. Peter, *ACS Appl. Mater. Inter.*, 2017, **9**, 3602-3615.
36. S. Kostera, B. Wyrzykiewicz, P. Pawluć and B. Marciniec, *Dalton Trans.*, 2017, **46**, 11552-11555.
37. P. Liu, C. Li and E. J. M. Hensen, *Chem.-Eur. J.*, 2012, **18**, 12122-12129.
38. P. Sudarsanam, A. Rangaswamy and B. M. Reddy, *RSC Adv.*, 2014, **4**, 46378-46382.
39. R. D. Patil and S. Adimurthy, *RSC Adv.*, 2012, **2**, 5119-5122.
40. A. Dhakshinamoorthy, M. Alvaro and H. Garcia, *ChemCatChem*, 2010, **2**, 1438-1443.
41. J. Jin, C. Yang, B. Zhang and K. Deng, *J. Catal.*, 2018, **361**, 33-39.
42. J. Yang and C.-Y. Mou, *Appl. Catal. B-Environ.*, 2018, **231**, 283-291.
43. A. Goto, H. Naka, R. Noyori and S. Saito, *Chem.-Asian J.*,

2011, **6**, 1740-1743.
44.K. Singh, A. Sarbajna, I. Dutta, P. Pandey and J. K. Bera, *Chem.-Eur. J.*, 2017, **23**, 7761-7771.
45.J. Long, K. Shen and Y. Li, *ACS Catal.*, 2017, **7**, 275-284.
46.M. K. Rong, K. van Duin, T. van Dijk, J. J. M. de Pater, B.-J. Deelman, M. Nieger, A. W. Ehlers, J. C. Slootweg and K. Lammertsma, *Organometallics*, 2017, **36**, 1079-1090.
47.N. Salam, S. K. Kundu, R. A. Molla, P. Mondal, A. Bhaumik and S. M. Islam, *RSC Adv.*, 2014, **4**, 47593-47604.
48.J. Zhang, J. Yang, J. Wang, H. Ding, Q. Liu, U. Schubert, Y. Rui and J. Xu, *Mol. Catal.*, 2017, **443**, 131-138.
49.X. Cui, Y. Long, X. Zhou, G. Yu, J. Yang, M. Yuan, J. Ma and Z. Dong, *Green Chem.*, 2018, **20**, 1121-1130.
50.J. Liang, X. Zhang, L. Jing and H. Yang, *Chin. J. Catal.*, 2017, **38**, 1252-1260.
51.X. Wang, X. Huang, W. Gao, Y. Tang, P. Jiang, K. Lan, R. Yang, B. Wang and R. Li, *J. Mater. Chem. A*, 2018, **6**, 3684-3691.
52.I. S. Pieta, A. Rathi, P. Pieta, R. Nowakowski, M. Hołdynski, M. Pisarek, A. Kaminska, M. B. Gawande and R. Zboril, *Appl. Catal. B-Environ.*, 2019, **244**, 272-283.
53.M. J. Lima, A. M. T. Silva, C. G. Silva and J. L. Faria, *J. Catal.*, 2017, **353**, 44-53.
54.X. Hu, Y. Long, M. Fan, M. Yuan, H. Zhao, J. Ma and Z. Dong, *Appl. Catal. B-Environ.*, 2019, **244**, 25-35.
55.Y. Zheng, L. Lin, X. Ye, F. Guo and X. Wang, *Angew. Chem. Int. Ed.*, 2014, **53**, 11926-11930.
56.T. S. Miller, A. B. Jorge, T. M. Suter, A. Sella, F. Cora and P. F. McMillan, *Phys. Chem. Chem. Phys.*, 2017, **19**, 15613-15638.
57.L. Xu, J. Xia, H. Xu, S. Yin, K. Wang, L. Huang, L. Wang and H. Li, *J. Power Sources*, 2014, **245**, 866-874.
58.S. Ren, C. Chen, Y. Zhou, Q. Dong and H. Ding, *Res. Chem. Intermediat.*, 2016, **43**, 3307-3323.
59.X. Fu, S. Wu, Z. Li, X. Yang, X. Wang, L. Peng, J. Hu, Q. Huo, J. Guan and Q. Kan, *RSC Adv.*, 2016, **6**, 57507-57513.
60.H.-C. Ma, J.-L. Kan, G.-J. Chen, C.-X. Chen and Y.-B. Dong, *Chem. Mater.*, 2017, **29**, 6518-6524.
61.K. Umemura, A. Takahashi and S. Kawai, *J. Wood Sci.*, 1998, **44**, 204-210.
62.T. Sun, H.-Y. Jiang, C.-C. Ma, F. Mao and B. Xue, *Catal. Commun.*, 2016, **79**, 45-48.
63.D. Roşu, F. Mustaă and C. N. Caşcaval, *Thermochim. Acta*, 2001, **370**, 105-110.
64.K. S. Anseth, C. M. Wang and C. N. Bowman, *Macromolecules*, 1994, **27**, 650-655.
65.P. Jiang, X. Li, W. Gao, X. Wang, Y. Tang, K. Lan, B. Wang and R. Li, *Catal. Commun.*, 2018, **111**, 6-9.
66.S. Frindy, A. Primo, H. Ennajih, A. El Kacem Qaiss, R. Bouhfid, M. Lahcini, E. M. Essassi, H. Garcia and A. El Kadib, *Carbohydr. Polym.*, 2017, **167**, 297-305.
67.F. Sun, H. Wu, X. Liu, F. Liu, H. Zhou, J. Gao and Y. Lu, *Nano Res.*, 2016, **9**, 3209-3221.
68.Z. Liu, F. Sun, L. Gu, G. Chen, T. Shang, J. Liu, Z. Le, X. Li, H. B. Wu and Y. Lu, *Adv. Energy Mater.*, 2017, **7**, 1701154.
69.K. Wang, W. Gao, P. Jiang, K. Lan, M. Yang, X. Huang, L. Ma, F. Niu and R. Li, *Mol. Catal.*, 2019, **465**, 43-53.
70.A. Grirrane, A. Corma and H. Garcia, *J. Catal.*, 2009, **264**, 138-144.
71.Z. Zhang, F. Wang, M. Wang, S. Xu, H. Chen, C. Zhang and J. Xu, *Green Chem.*, 2014, **16**, 2523-2527.
72.Y. Wang, J. Zhou, X. Hao, Y. Wang and Z. Zou, *Appl. Surf. Sci.*, 2018, **456**, 861-870.
73.L. Jiang, L. Jin, H. Tian, X. Yuan, X. Yu and Q. Xu, *Chem. Commun.*, 2011, **47**, 10833-10835.
74.B. Zhu, M. Lazar, B. G. Trewyn and R. J. Angelici, *J. Catal.*, 2008, **260**, 1-6.
75.N. Kang, J. H. Park, K. C. Ko, J. Chun, E. Kim, H.-W. Shin, S. M. Lee, H. J. Kim, T. K. Ahn, J. Y. Lee and S. U. Son, *Angew. Chem. Int. Ed.*, 2013, **52**, 6228-6232.
76.G. Yuan, M. Gopiraman, H. J. Cha, H. D. Soo, I.-M. Chung and I. S. Kim, *J. Ind. Eng. Chem.*, 2017, **46**, 279-288.
77.M. Gopiraman and I. M. Chung, *J. Taiwan Inst. Chem. E.*, 2017, **81**, 455-464.